

Thermal Ageing in Continuous Basalt Glass Fibres

Yuanzheng Yue

Aalborg University, Fibigerstraede 16, DK-9220 Aalborg Øst, Denmark

Søren Lund Jensen

Rockwool International A/S, Hovedgaden 584, DK-2640 Hedehusene, Denmark

To understand the relaxation mechanism of the inorganic glass below the glass transition temperature (T_g), physical ageing experiments on the continuous basalt fibres are conducted in a temperature range from $0.55T_g$ to $0.95T_g$, where T_g is 908K. The rate of energy release from the fibres as a function of temperature is determined by using a differential scanning calorimeter (DSC). The average fictive temperature of the non-aged fibres cooled with about 10^5 K/s is found to be $1.19T_g$. During heating of the aged fibres, a relaxation endotherm occurs followed by an exotherm. When increasing the ageing temperature, the endotherms become more pronounced and shifts to higher temperatures, accompanied by a gradual disappearance of the exotherm. The fact that the energy release occurs in a large temperature range suggests that a hyperquenched glass fibre possesses a large distribution of excess energy over all configurational coordinates and, hence, a large diversity of the frozen structural rearrangement. The co-existence of the endotherms and exotherms indicates that two spectra of fictive temperatures exist in the structure of the aged fibres. A phenomenological equation has been proposed to describe the decrease of the remaining energy with increasing ageing temperature.

Introduction

When a glass-forming liquid is cooled with the rate 10 K/min, the glass transition occurs around the temperature corresponding to the viscosity 10^{12} Pa s. This temperature is normally refers to as the glass transition temperature (T_g). If the liquid is hyperquenched (e.g. with the rate of 10^5 K/s), the glass transition will occur at a temperature that is much higher than T_g . This temperature is called the fictive temperature (T_f). Narayanaswamy¹ proposed a phenomenological model that describes the structural relaxation behaviour of glass. In the past three decades, this model has been widely and successfully used for a better understanding of the glass transition and for a better design of the annealing and tempering processes. Recently, it has, however, been realised that Narayanaswamy's model is not suitable for describing the enthalpy relaxation of hyperquenched glasses (e.g. thin glass fibres)^{2,3} and especially in representing the temperature dependence of the heat capacity of the fibres aged at temperatures below T_g ⁴.

Physical ageing exerts a strong and complex impact on properties of glasses. It should be noted that substantial work has been done on physical ageing in organic glasses well below T_g by means of the differential scanning calorimeter (DSC)^{5,6,7}. Much less investigations have, however, not been carried out on hyperquenched glass fibres. Most recently, some work on the physical ageing of basaltic glass wool, i.e. discontinuous fibres with high T_f ($=1.22T_g$), has been done by the present authors⁸. In this paper, systematic calorimetric experiments have been performed on the continuous basaltic fibres aged for three hours at temperatures between $T_a = 0.55T_g$ and $0.95T_g$. The complexity of enthalpy relaxation is demonstrated on the aged fibres. The experimental data can contribute to exploring the origin of superior physical properties of fibres over those of the slowly cooled glass. They can also be used for finding a more general phenomenological model to describe the relaxation behaviour of

both slowly cooled and hyperquenched glasses⁴. Finally, this study gives a new insight into the energy landscape of glass-forming liquids.

Experimental

Fibres were continuously drawn from a basalt glass melt with the composition: 49.3 SiO₂, 15.6 Al₂O₃, 1.8 TiO₂, 11.7 FeO, 10.4 CaO, 6.6 MgO, 3.9 Na₂O, and 0.7 K₂O (wt%) at the temperature 1420 K by using a platinum crucible with a die (2 mm in diameter). The fibres are cooled with a rate of about 10⁵ K/s. The diameter of the fibres is about 9.2 μ m.

The heat capacity of the fibers was measured using a differential scanning calorimeter (DSC) Netzsch STA 449C. The fibers were placed into a platinum crucible situated on a sample holder of the DSC at room temperature. The fibers were heated to $T = 993$ K and, afterwards cooled to room temperature. Both the heating and cooling rates were 0.333 K/s. To determine the heat capacity (C_p) of the fibers, both the baseline (blank) and the reference sample (Sapphire) were measured. Ageing of the fibres is performed in air at various temperatures for 3 hours. The fibres were subjected to two upscans. The first upscan was made on an unrelaxed sample, whereas the second was performed on the sample relaxed due to the first upscan.

T_g was found to be 908 K from the C_p curve of the second upscan with the heating rate 0.167 K/s. Before the second upscan, each sample was cooled at 0.167 K/s. T_f of the non-aged fibres was found to be 1084 K by using a newly proposed approach⁹.

Results and Discussion

Figure 1a shows the heat capacity curve of both non-aged and aged fibres. C_{p1} and C_{p2} represents the heat capacities measured on the first and second runs of DSC upscans, respectively. T_c is the onset temperature, at which the enthalpy starts to release, meaning that the fictive temperature begins to drop. The T_c value of the fibres aged for 3 hours at 683 K is higher than that of the non-aged fibres. The former and latter are 726 K and 550 K, respectively. Figure 1b is obtained from figure 1a, which demonstrates the rate of the energy release of the continuous basalt fibres, $d\Delta E/dT = C_{p2} - C_{p1}$, as function of temperature T . The $d\Delta E/dT$ value is the energy released from one gram fibres per one Kelvin, where $\Delta E(T)$ is the total excess energy released during heating to a given T . In this work, $d\Delta E/dT$ is treated as the rate of energy release from fibres, because of the relation $d\Delta E/dT = d\Delta E/(Q_h dt)$, where Q_h is a constant heating rate 0.333 K/s. The total energy stored in the fibres during fibre drawing process, ΔE_{tot} , is calculated by integrating $d\Delta E/dT$ over the entire temperature range between the onset temperature of the non-aged fibres (T_{c1}) and the onset temperature for their structural equilibrium (T_e). The energy (ΔE_{rem}) remaining in fibre after 3 hours of ageing is estimated by integrating $d\Delta E/dT$ over the temperature range between T_{c2} and T_e .

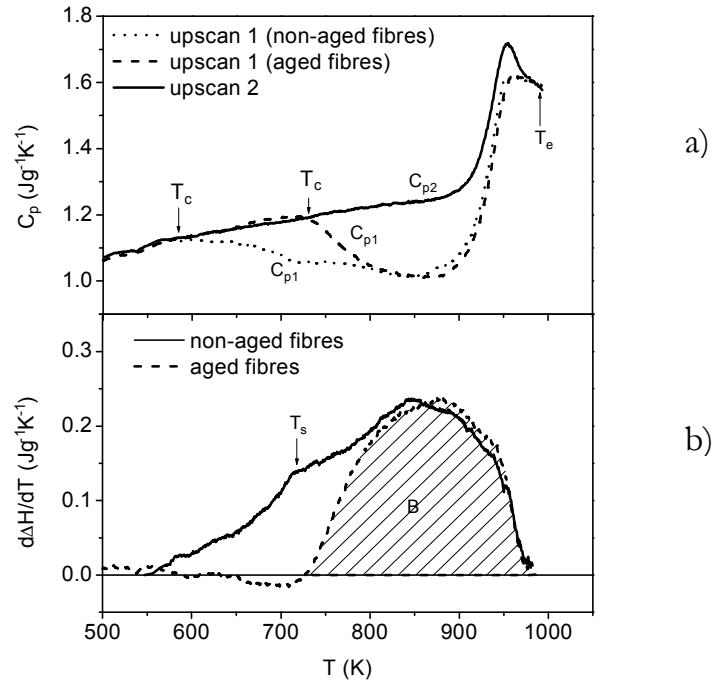


Figure 1 The energy release from both the non-aged and aged fibres during DSC upscans as function of temperature. Both heating and cooling rates used for the DSC measurements are 0.333 K/s. **a)** The heat capacity curves measured by the first upscan (C_{p1}) and by the second upscan (C_{p2}). The dashed line represents the C_p curve of the sample aged for 3 hours at 683 K. **b)** The rate of energy release, $d\Delta E/dT$, that is, $C_{p2} - C_{p1}$. Area B stands for the excess energy remaining after 3 hours of ageing at 683 K.

From figure 1b it can be seen that a 'shoulder' appears on the energy release curve of the non-aged fibres at $T_s = 0.78T_g$. The existence of the 'shoulder' implies an overlap of two relaxation processes of the fibres. The distribution of $d\Delta E/dT$ over T is not symmetric, and a long tail is observed at the lower temperature range above T_c . The main peak in the high temperature domain is associated with structural transformations with a smaller departure from the equilibrium and with a smaller potential energy compared to the other observed at low temperatures near T_s . Thus, these regimes require high thermal excitation energy to approach the states, which are determined by both the heating rate and temperature. These structural regions may be related to the structural network consisting of the $[\text{SiO}_4]$ and $[\text{AlO}_4]$ tetrahedra, the bonds of which are energetically much more stable than the bonds between glass modifiers and non-bridging oxygen ions. The shoulder could be associated with transformations of domains, where the glass modifiers suffer more strain. After 3 hours of ageing at 683 K, the high excess energy part of the structure relaxes due to the thermal excitation related to the low temperatures range from T_{c1} to T_{c2} . The relaxation of the low excess energy part of the structure occurring in the high temperature range from T_{c2} to T_e is detected during the first DSC upscan (see the hatched area of figure 1).

Figure 2 illustrates the effect of the ageing temperature on energy release behaviour. When increasing the ageing temperature (T_a), the exotherm is gradually reduced from the left side to the right, until it totally disappears. Consequently, the onset temperature (T_c) shifts to higher temperatures. This phenomenon reflects a large distribution of deepness of the minima which the system explores on the energy landscape at $T_f = 1084$ K. Thus, a large diversity of configurational states exists in the melt at 1084 K. During the ageing process, the structural configuration with a higher energy is transformed into that with a lower energy. The ageing temperature determines the extent of changes in the structural configuration. The vibrational excitation energy required for the change in the structural configuration depends on its energy level. The final goal of all configurational states is to reach the energy level corresponding to the ageing temperature. The shift of T_c to higher temperatures is due to the fact that more and more low energy basins of the energy landscape are sampled by the system when increasing the ageing temperature.

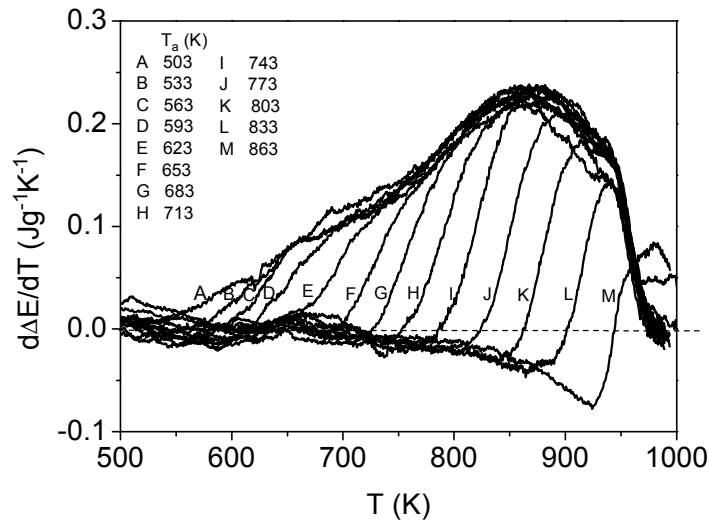


Figure 2 The rate of energy release from the fibres, $d\Delta E/dT$, of fibres aged for 3 hours at different temperatures (T_a). The heating and cooling rates are 0.333 K/s.

Figure 2 demonstrates that a relaxation endotherm occurs above certain temperatures, which is connected with the left foot of the exotherm. The higher the ageing temperature is, the deeper and the broader the endotherms become. At the same time, the endotherm gradually shifts to higher temperatures, but at the cost of successive loss of the left part of the exotherm. In a certain range of ageing temperatures, the exotherm and endotherm co-exist. This again suggests that there are different structural domains in the fibres and, hence, in the melt at $T = T_f$. In other words, the topographical arrangement of structure in the fibres is different from one domain to another. However, these structural domains are interconnected, because energy release proceeds continuously with increasing ageing temperature and the two distributions of $d\Delta E/dT$ over T (see the exothermic ‘shoulder’ and main peak in figure 1b) are overlapped to great extent. The same inference was obtained from the study of the physical ageing of the discontinuous fibres⁸. The fact that the endotherm becomes deeper with increasing T_a means that the difference of T_f from T_a is getting smaller. Above T_g , T_f is equal to T_a .

Figure 3 demonstrates the T_a dependence of the remaining energy (ΔE_{rem}) normalised by the total energy (ΔE_{tot}) for the given ageing time 3 hours. This experimental dependence can be fitted by the equation:

$$\frac{\Delta E_{\text{rem}}}{\Delta E_{\text{tot}}} = \left(\frac{T_r}{T_a}\right)^c (1 - \exp(-(\frac{T_a}{T_r})^c))$$

where T_r is a characteristic temperature, at which $\Delta E_{\text{rem}}/\Delta E_{\text{tot}} = 0.63$, and c is the stretch or shape parameter, which reflects the sensitivity of the remaining energy ΔE_{rem} to the ageing temperature. The bigger the c value is, the faster the remaining energy ΔE_{rem} decreases with increasing T_a . In other words, the bigger the c value, the steeper the $\Delta E_{\text{rem}}/\Delta E_{\text{tot}} \sim T_a$ curve. The T_r and c parameters depend on both composition and forming conditions of glass fibres¹⁰. Both decrease with increasing ageing time¹⁰. In the present work, $T_r = 723$ K and $c = 13$. From about 600 K on, ΔE_{rem} starts to drop dramatically. Each ageing temperature is associated with a set of structural relaxation time spectra, since relaxation time is distributed in more than one spectrum for most of amorphous materials.

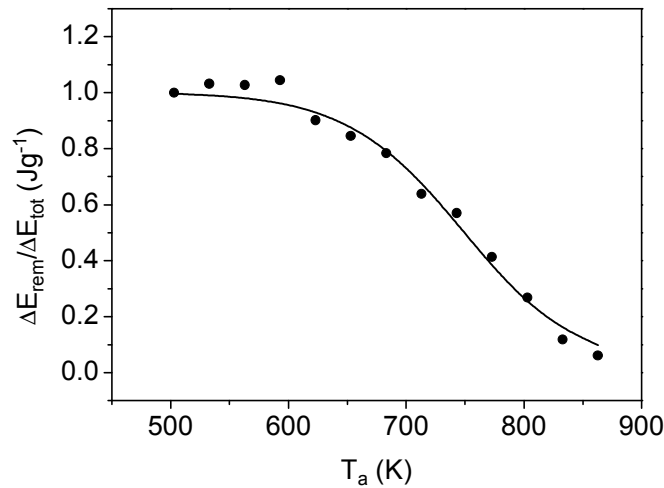


Figure 3 The remaining energy normalised by the total energy stored during forming of the fibres, $\Delta E_{\text{rem}}/\Delta E_{\text{tot}}$, versus the ageing temperature T_a . ΔE_{tot} is obtained by calculating the area surrounded by the C_{p1} and C_{p2} curves of the non-aged fibres (see figure 1). The solid line is obtained by fitting the experimental data to equation 1.

Summary

The energy release occurs in a large temperature range from $0.55T_g$ to T_g . This implies that a hyperquenched fibre possesses a large distribution of the excess energy and, hence, a large diversity of the frozen structural rearrangement over all configurational coordinates. The existence of the ‘shoulder’ on the energy release curve indicates that at least two major relaxation time spectra exist, each of which is attributed to an independent structural domain. The onset temperature, at which the energy release starts during the first DSC upscans, shifts to higher temperature with increasing the ageing temperature for a given

ageing time interval. The co-existence of the endotherms and exotherms indicates that two spectra of fictive temperatures exist in the structure of the aged fibres.

A phenomenological equation has been proposed to describe the decrease in the remaining energy with increasing ageing temperature. Two parameters (T_s and c) determine the dependence of the remaining energy. In terms of the two parameters, the structural relaxation and physical properties of glass fibres can be characterised, which depend on the chemical composition and forming conditions.

Acknowledgments

The authors would like to thank C. A. Angell, T. Knudsen and J. deC. Christiansen for valuable discussions. This work was financially supported by the Rockwool International A/S.

¹ Q.S. Narayanaswamy, J. Am. Ceram. Soc. **54**, p. 491 (1971).

² J. Huang and P. K. Gupta, J. Non-Cryst. Solids **151**, p. 175 (1992).

³ J.P. Ducroux, S.M. Rekhson and F.L. Merat, J. Non-Cryst. Solids **172-174**, p. 541 (1994).

⁴ T. Knudsen, Rockwool International A/S, private communication

⁵ I.M. Hodge, Science **267**, p. 1945 (1995)

⁶ I.M. Hodge, J. Non-Cryst. Solids **169**, p. 211 (1994).

⁷ A. D. Drozdov, Euro. Polymer. J. **37**, p. 1379 (2001).

⁸ Y.Z. Yue, S.L. Jensen and J. deC. Christiansen (In publication).

⁹ Y.Z. Yue, J. deC. Christiansen and S.L. Jensen, Chemical Physics Letters (2002) (In press).

¹⁰ Y.Z. Yue, Research Report, Aalborg University, (2002).